

# Articles

## Low Strain Nanomechanics of Collagen Fibrils

August J. Heim,<sup>†</sup> Thomas J. Koob,<sup>‡</sup> and William G. Matthews<sup>\*,†</sup>

*Departments of Physics and Chemical Engineering, University of South Florida, 4202 East Fowler Avenue, Tampa, Florida 33620-5700*

*Received December 6, 2006; Revised Manuscript Received March 30, 2007*

The high stiffness of collagenous tissues such as tendon and ligament is derived in large part from the mechanics and geometries of the constituent collagen's hierarchical forms. The primary structural unit in connective tissues is the collagen fibril for which there exists little direct mechanical or deformational study. Therefore, the current understanding of the mechanisms involved is extrapolated from whole tissue data. To address this, the elastic response due to bending of readily extractable adult collagen fibrils was studied, and the results were compared to previously reported radial indentation experiments. A demonstration of a material anisotropy arising without loss of the assumptions of homogeneity is presented.

The bulk of animal connective tissues are based on collagen fibrils. Fibrils are high-aspect-ratio biopolymers based upon tropocollagen molecule monomers (length  $\approx 300$  nm and diameter  $\approx 1.5$  nm), which are laterally staggered in an almost crystalline structure. This structure creates an observable periodicity known as the d-band. Concomitant with other matrix proteins and elastic filaments, collagen fibrils reinforce tissue systems involved in compliance, structural support, and force transduction in motile organisms. Connective tissues are higher-ordered structures and are best described as biocomposites with the fibril providing the fibrous phase. A full description of fibril mechanics is important for proper modeling of connective tissues, both for biomaterial development and for an understanding of the pathologies of diseased and degenerative tissues. Currently, the properties of fibrils under load are ascertained from whole tissue data<sup>1</sup> and two isolated direct mechanical experiments<sup>2,3</sup> due to difficulty in isolation of native, precipitated *in vitro* fibrils from adult animals.

Recent mechanical testing performed on isolated high-aspect-ratio fibers with similar dimensions involved nanoscale three-point bending,<sup>4–6</sup> lateral force microscopy,<sup>7,8</sup> indentation,<sup>9,10</sup> and a mechanical strain apparatus.<sup>2</sup> These tests provide suitable means by which to study collagen fibrils under varying load geometries. The physical quantity measured in these experiments is the modulus corresponding to out-of-plane mechanical strain. In the case of isotropic materials, this modulus is the elasticity ( $E$ ); for anisotropic materials, it is a function of both in-plane shear ( $G$ ) and elasticity. For a polymer fiber with a solid cross-section, the previously reported modulus measured through both radial indentation and three-point bending agree within uncertainty, illustrating no anisotropy.<sup>6,9</sup> Alternatively, microtubules exhibited an anisotropy of structural nature in origin, related to their thin shell cross-section.<sup>4</sup>

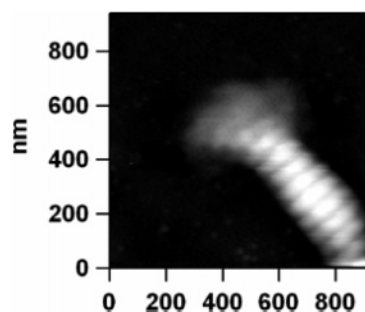


**Figure 1.** Collagen fibril fractured under shear during deposition. During high-shear events, pipetting or lateral force applied via contact AFM, collagen fibrils can be severed. The high internal strain gives rise to dispersion of the monomers and pinching at the sheared end.

Even though the fibrils are almost crystalline, there are strong arguments for an elastic anisotropy derived from shearing deformations of a thin shell around a less-ordered core,<sup>11</sup> which would lead to a decrease in the expected modulus as a function of fibril diameter. Additionally, an anisotropy is seen in the bulk collagen structures involved in articulation of joints.<sup>12</sup> An atomic force microscopy (AFM) image of collagen fibrils demonstrating the effect of strain relaxation on the fibril morphology is shown in Figure 1. The monomers swell and spread out at the fractured end of the fibril, forming a brush presumably resulting from internal strain and from high internal hydration pressure. Perhaps surprisingly, the d-banding is maintained throughout.

Fibril hydration creates an increase in fibril diameter of  $>50\%$  from in-house AFM observations (data not shown), demonstrating the presence of a matrix phase. This degree of expansion is not reflected in the longitudinal dimensions, which otherwise would appear as a significant lengthening of the d-band with increasing hydration. To determine the material properties inherent solely in the molecular structure, fibrils were tested in ambient air. Three-point bending measurements of collagen fibrils in air are representative of intrafibrillar shear, reorienta-

\* Author to whom correspondence should be addressed. E-mail: gmatthew@cas.usf.edu.

<sup>†</sup> Department of Physics.

<sup>‡</sup> Department of Chemical Engineering.

tion, and fibril elongation. Under the idealized assumptions of an isotropic homogeneous material, these measurements yield the elastic modulus, as is the case for deflections much less than the span length where the effects of shear are small. The validity of these assumptions can be confirmed by plotting modulus versus aspect ratio. To determine the effects of fibril ultrastructure on the material properties, the method of nanoscale three-point bending via AFM was applied, and the results were compared to previous studies of radial indentation of dehydrated collagen fibrils assumed to be solid cross-sectional cylinders. In the previous studies, the reduced modulus, defined as

$$E_r = E(1 - \nu^2)^{-1} \quad (1)$$

with  $E$  and  $\nu$  the Young's modulus and Poisson ratio, was determined to be  $\sim 1\text{--}2$  GPa<sup>13</sup> with no apparent correlation to fibril diameter. Using an assumed Poisson ratio of 0.3, this yields an elastic modulus of 0.9–1.8 GPa.

The collagen fibrils used were isolated from minced tissue of the ventral interambulacral region of a common sea cucumber, *Cucumaria frondosa*, and stored as an emulsion in water.<sup>14</sup> A standard AFM calibration grating with steps  $\sim 1.5\text{--}2$   $\mu\text{m}$  wide and 0.5  $\mu\text{m}$  deep was used as beam supports for three-point bending experiments. The SiN<sub>3</sub> surface was functionalized either by (1) vapor depositing hexamethyldisilazane (HMDS) under ambient pressure, producing a methyl-terminated monolayer and rendering the grating hydrophobic, or by (2) depositing (3-aminopropyl) triethoxysilane (APTES) diluted in ethanol, producing an amino-terminated monolayer. Both electrostatic interactions between the highly sulfated glycosaminoglycan and the APTES surface and hydrophobic interactions with the HMDS surface were found to sufficiently secure fibrils to the surface as verified through contact mode AFM (see next paragraph). While the mechanism is not well understood, it has been commonly observed that fibrils adhere to surfaces of increasing hydrophobicity.

Fibrils were deposited from an emulsion in water onto a glass slide that previously had been plasma-cleaned to render the surface hydrophilic and induce wetting. The grating then was allowed to sit inverted and covered for 1–2 h on the glass slide. This two-step procedure was designed to minimize the fibrils' tendency to conform to the contours of the grating. The sample was then washed with copious amounts of water followed by nitrogen drying. As determined from imaging under minimal applied load (maintaining a high set point  $>85\%$  of the free amplitude), occasionally fibrils tautly and orthogonally span the grating gap (Figure 2). Contact scans transverse to the fibril axis under high applied forces were unable to displace the fibrils and often cut the fibril before any detectable lateral changes in position occur, providing evidence for strong surface immobilization.

Bending experiments were performed using cantilevers with spring constants between 1 and 20 nN/nm. The apical radius, determined from deconvolution of imaging data, was on the order of 10–100 nm for each experiment. The spring constants were calibrated using thermal resonant frequency analysis and the Sader method<sup>15</sup> and were within manufacture's specifications. Calibration of the piezo response was accomplished by performing a force curve on surfaces (silicon or glass) hard relative to the collagen fibrils.

The central displacement of a suspended beam under central loading is given by

$$\delta = \delta_{\text{bending}} + \delta_{\text{shear}} = FL^3/192EI + f_s FL/4GA \quad (2)$$

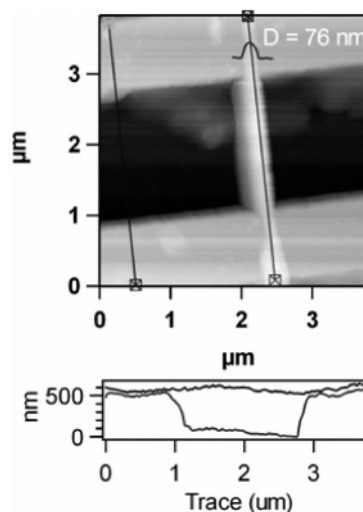


**Figure 2.** Suspended collagen fibril (top panel) and sectional traces (bottom panel). The fibril can be seen to be tautly bound and orthogonal to the gap. The AFM image was obtained at very low setup amplitude damping to minimize fibril deflection during the scan.

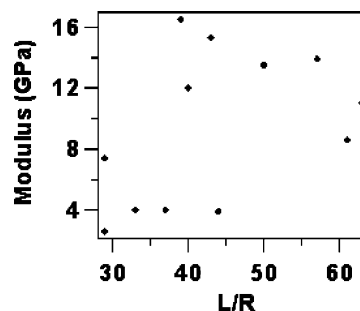


**Figure 3.** Plot of  $E_{\text{bending}}$  (as derived through eq 2) vs  $L/R$  demonstrating minimal correlation. It would be expected to see a strong decreasing trend if shear is constituent in bending mechanics.

where  $L$  is the span length,  $E$  the elastic modulus,  $G$  the shear modulus,  $I$  the second moment of area equal to  $\pi D^4/64$ , and  $f_s$  a constant dependent upon geometry of the beam (10/9 for a cylinder<sup>16</sup>). The factor  $\delta_{\text{bending}}/\delta_{\text{shear}}$  increases with ratio of span length to beam diameter, leading to negligible shear effects for  $L/R > 4\sqrt{E/G}$ .<sup>17</sup> The gap spacing of the grating used and the average fibril diameter of  $<150$  nm allow this ratio to be maintained well above the threshold where shear can be assumed small. The average deflection was maintained on the order of the fibril diameter or smaller to minimize shear. Additionally,  $E_{\text{bending}}$  versus  $L/R$  is plotted in Figure 3, and no decreasing trend is observed, confirming the lack of shear effects. Under these conditions the second term in eq 2 above can be ignored.

Fourteen AFM force curves deflecting different suspended fibrils were recorded. A sample force curve is shown in Figure 4. The recorded data was truncated and fit to the general beam theory outlined above and is presented in Figure 5 as a plot of modulus versus fibril diameter. This analysis yielded a mean bending modulus of  $10.0 \pm 5$  GPa. In a theoretical study, Vesentini found a modulus value for collagen-like homotrimers (*C. frondosa* fibrils are homotrimers) to be around 2 GPa.<sup>18</sup> The previously reported modulus of hydrated collagen fibrils under high strain was estimated to be 12 GPa and, for low strain, 0.5 GPa.<sup>2</sup> As pointed out by the authors, both values are based on diameters measured on dehydrated fibrils, likely producing inflated numbers. Since the measurements herein are dehydrated, we expect only to be comparable to the high strain modulus of 12 GPa. At high strain, the collagen fibrils may be acting as a composite with a minimal matrix phase component, having shed

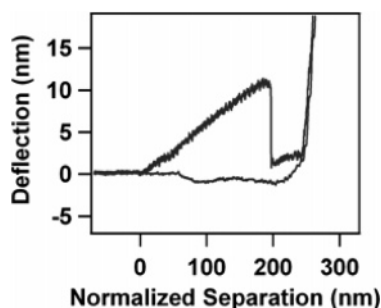


**Figure 4.** Typical AFM cantilever deflection vs separation plot during a load/unload cycle. Between a separation of 0 and ~200 nm the linearity expected in Euler–Bernoulli beam theory can be observed. After ~12 nm of deflection (at ~200 nm separation), the tip–fibril contact was lost. The slight negative deflection of the cantilever is likely due to friction between the side of the tip and the suspended fibril.

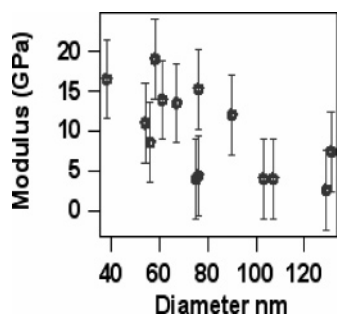


**Figure 5.** Plot of  $E_{\text{bending}}$  vs diameter for fibril bending demonstrating, within uncertainty, no correlation between fibril diameter and modulus.

intrafibrillar water molecules due to increasing constriction of semibraided monomers.<sup>19</sup> Similarly, loss of viscoelasticity is attributable to less hydrogen bonding. Under these conditions the previously reported values agree well with those reported here.

The power law dependencies of the modulus on fibril diameter and suspended length make the measurement error sensitive to these terms. Taking that the error in measurement of the span length and fibril diameter of ~10%, which can cause error in the Euler–Bernoulli beam formulation and that this error in  $D$  and  $L$  is independent and random, the sum of all propagated error is <50%. On the basis of this variation and the probable increase in minor tip indentation into larger fibrils contributing to a lower apparent modulus, the plot shows little correlation ( $r$  value of  $-0.659$ ) between  $E_{\text{bending}}$  and beam diameter in Figure 5. Unlike in the present case, the effects of shear on the reported modulus previously have shown an order of magnitude change in the bending modulus over small increases in nanofiber diameter.<sup>17</sup> Classical nonconservative models with slip and without the assumption of a high static frictional component would yield increased values for the modulus. Similarly, the moment of inertia for a hollow, or inhomogeneous cylinder, is lower than that of a solid cylinder of identical outer diameter. Thus, the expected modulus reported in this analysis is a conservative lower bound.

For comparison with other nanometer scale dimension filaments, moduli for multiwall carbon nanotubes<sup>20</sup> ( $r \approx 30$  nm) and Si<sup>5</sup> and Au nanowires<sup>7</sup> ( $r \approx 50$  nm) previously have been reported. The Young's moduli of these materials were between 16 and 80 GPa. Force microscopy on bacteriophage capsids, which are biocomposites, yielded 1.8 GPa.<sup>21</sup> The herein reported dehydrated material properties place cucumber fibrils among the stiffest eukaryotic biomaterials, though not studied in its native environment.

The lack of shear result predicts dehydrated collagen fibrils to be isotropic and homogeneous. However, in comparing our current results from three-point bending with the previously reported radial indentation data,<sup>13</sup> there appears to be a nearly ~10-fold anisotropy. In a recent related study on cortical bone, Fan et al. measured the effect of anisotropy on indentation and found a ~30% variance as a function of load angles,<sup>22</sup> significantly less than the variation observed in our studies on individual fibrils.

Recent second harmonic imaging of collagen suspensions<sup>23</sup> and electron microscopy images<sup>19</sup> lead us to propose that the fibril anisotropy is due to constriction or breathing of intertwined or braided collagen monomers within the microfibrillar unit. Tropocollagen molecules often are considered as rigid rods in tissue systems and display very low strains of failure relative to higher-ordered collagen structures;<sup>24</sup> bulk collagenous tissues fail at higher strains. This effect must be correlated to the three-dimensional structure of the monomers in the fibril unit and, similarly, of the fibril unit in higher-ordered forms, i.e., the crimp in fibers. We propose that, by the twisting of collagen monomers at a loss of rigidity, an increase in strains of failure in the fibril will result. This conclusion would purport that single-fibril-supported composite materials would demonstrate a triphasic stress/strain behavior consisting of initial molecular alignment directed along the fibril axis, followed by linear elastic “stretching” of the fibril/matrix composite, and, finally, induced plasticity. Unlike fibrinogen<sup>8</sup> (a similar hierarchical protein), collagen fibrils are not pliable due to monomer structure but due to relaxation of wrapped collagen molecules. Since fully hydrated fibrils tolerate larger perturbations due to microfibril expansion, under hydrated conditions it is expected that, under limited deflection, this constriction/relaxation phenomenon will dominate the material properties. Sasaki reported that a fibril strain of 2% was 85% molecular elongation and 15% molecular rearrangement but did not consider constriction of helicity.<sup>1</sup>

Modeling of a fibril is best described as a two-phase, discretely reinforced fibrous composite with a loss factor applied to the monomer modulus due to wrapping in the microfibril. We propose the following modified form of the Halpin–Tsai result, which can be inverted to extract the monomer modulus from in situ physiological testing

$$E_c = E_m \frac{1 + f(A, \phi) V_f}{1 - f(A, \phi) V_v} \quad (3)$$

where  $E_c$  is the composite modulus,  $E_m$  is the monomer modulus,  $V_f$  and  $V_v$  are respective volume fractions of fiber and matrix phases, and  $f$  is a function of known helicity  $\phi$  and aspect ratio  $A$ . This constriction/relaxation model explains the discrepancy in the stress/strain relationship between deformation mechanics of fibrils studied in bulk tissues by X-ray diffraction<sup>1</sup> and those studied by tensile testing.<sup>2</sup> Loads that align the tendonal crimp are insufficient to elongate the semibraided microfibril, so analysis of whole tissue data reports a linear stress/strain relationship, whereas direct fibril measurements illustrate a so-called toe region. From braid theory, a twisting of the fiber phase lessens the fibril modulus as a function of assumed pitch angle and is given by the function

$$\frac{E_{\text{fibril}}(3 \sin^2 \theta)}{2 \sec^2 \theta - 1} \quad (4)$$

Combining this equation with the Halpin–Tsai result along with a known aspect ratio (tropocollagen  $D \approx 1.5$  nm and  $L \approx 300$

nm), a value for  $E_c < 500$  MPa,<sup>2</sup> and the modulus of the matrix phase of 1.6 MPa,<sup>25</sup> a lower bound for the expected monomer modulus can be obtained. This monomer modulus is  $\sim 5$  GPa, in line with published values.<sup>1,26</sup> The elastic energy storage can be explained simply by considering the geometry of the fibrils within microfibril units.

In conclusion, novel nanoscale bending of native, adult collagen fibrils was performed, the results of which demonstrated a  $\sim 10$ -fold material anisotropy. We conjecture that this anisotropy is related to relaxation of monomers intertwined in microfibrils rather than shear.

**Acknowledgment.** This work was supported by a National Science Foundation Integrative Graduate Education and Research Traineeship (Grant No. DGE 0221681).

## References and Notes

- (1) Sasaki, N.; Odajima, S. *J. Biomech.* **1996**, 29, 1131.
- (2) Eppell, S. J.; Smith, B. N.; Kahn, H.; Ballarini, R. *J. R. Soc. Interface* **2006**, 3, 117.
- (3) Graham, J. S.; Vomund, A. N.; Phillips, C. L.; Grandbois, M. *Exp. Cell. Res.* **2004**, 299, 335.
- (4) Kis, A.; Kasas, S.; Babić, B.; Kulik, A. J.; Benoît, W.; Briggs, G. A.; Schönenberger, C.; Catsicas, S.; Forró, L. *Phys. Rev. Lett.* **2002**, 89, 248101.
- (5) Ni, H.; Li, X.; Gao, H. *Appl. Phys. Lett.* **2006**, 88, 043108.
- (6) Tan, E. P. S.; Lim, C. T. *Appl. Phys. Lett.* **2004**, 84, 1603.
- (7) Wu, B.; Heidelberg, A.; Boland, J. J. *Nat. Mater.* **2005**, 4, 525.
- (8) Liu, W.; Jawerth, L. M.; Sparks, E. A.; Falvo, M. R.; Hantgan, R. R.; Superfine, R.; Lord, S. T.; Guthold, M. *Science* **2006**, 313, 634.
- (9) Tan, E. P. S.; Lim, C. T. *Appl. Phys. Lett.* **2005**, 87, 123106.
- (10) de Pablo, P. J.; Schaap, I. A.; MacKintosh, F. C.; Schmidt, C. F. *Phys. Rev. Lett.* **2003**, 91, 098101.
- (11) Gutsman, T.; Fantner, G. E.; Venturoni, M.; Ekani-Nkodo, A.; Thompson, J. B.; Kindt, J. H.; Morse, D. E.; Fygenson, D. K.; Hansma, P. K. *Biophys. J.* **2003**, 84, 2593.
- (12) Bennett, M. B.; Ker, R. F.; Dimery, N.; Alexander R. M. *J. Zool.* **1986**, 209, 537.
- (13) Heim, A. J.; Matthews, W. G.; Koob, T. J. *Appl. Phys. Lett.* **2006**, 89, 181902.
- (14) Trotter, J. A.; Lyons-Levy, G.; Thurmond, F. A.; Koob, T. J. *Comp. Biochem. Physiol., Part A: Physiol.* **1995**, 112, 463.
- (15) Sader, J. E.; Chon, J. W. M.; Mulvaney, P. *Rev. Sci. Instrum.* **1999**, 70, 3967.
- (16) Timoshenko, S. P.; Gere, J. M. *Mechanics of Materials*; Van Nostrand Reinhold: New York, 1972.
- (17) Salvétat, J.-P.; Briggs, G. A. D.; Bonard, J.-M.; Bacsá, R. R.; Kulik, A. J.; Stöckli, T.; Burnham, N. A.; Forró, L. *Phys. Rev. Lett.* **1999**, 82, 944.
- (18) Vesentini, S.; Fitié, C. F. C.; Montevecchi, F. M.; Redaelli, A. *Biomech. Model. Mechanobiol.* **2005**, 3, 224.
- (19) Orgel, J. P. R. O.; Irving, T. C.; Miller, A.; Wess, T. J. *Proc. Natl. Acad. Sci. U.S.A.* **2006**, 103, 9001.
- (20) Yu, M.-F.; Lourie, O.; Dyer, M. J.; Moloni, K.; Kelly, T. F.; Ruoff, R. S. *Science* **2000**, 287, 637.
- (21) Ivanovska, I. L.; de Pablo, P. J.; Ibarra, B.; Sgalari, G.; MacKintosh, F. C.; Carrascosa, J. L.; Schmidt, C. F.; Wuite, G. J. L. *Proc. Natl. Acad. Sci. U.S.A.* **2004**, 101, 7600.
- (22) Fan, Z.; Swanener, J. G.; Rho, J. Y.; Roy, M. E.; Pharr, G. M. *J. Orthop. Res.* **2002**, 20, 806.
- (23) Williams, R. M.; Zipfel, W. R.; Webb, W. W. *Biophys. J.* **2002**, 82, 175A.
- (24) Sasaki, N.; Odajima, S. *J. Biomech.* **1996**, 29, 655.
- (25) Freeman, J. W.; Silver, F. H. *J. Theor. Biol.* **2004**, 229, 371.
- (26) Lorenzo, A. C.; Caffarena, E. R. *J. Biomech.* **2005**, 38, 1527.

BM061162B